



Setting up tracking tools for NuFact bowtie decay ring studies

D. Kelliher, F. Lemuet, F. Méot, G. Rees

► To cite this version:

D. Kelliher, F. Lemuet, F. Méot, G. Rees. Setting up tracking tools for NuFact bowtie decay ring studies. 2006, 11 p. in2p3-00140477

HAL Id: in2p3-00140477

<https://hal.in2p3.fr/in2p3-00140477>

Submitted on 6 Apr 2007

HAL is a multi-disciplinary open access archive for the deposit and dissemination of scientific research documents, whether they are published or not. The documents may come from teaching and research institutions in France or abroad, or from public or private research centers.

L'archive ouverte pluridisciplinaire **HAL**, est destinée au dépôt et à la diffusion de documents scientifiques de niveau recherche, publiés ou non, émanant des établissements d'enseignement et de recherche français ou étrangers, des laboratoires publics ou privés.

Setting up tracking tools for NuFact bowtie decay ring studies

D. Kelliher^{*}, F. Lemuet[†], F. Méot[‡], G. Rees^{*}

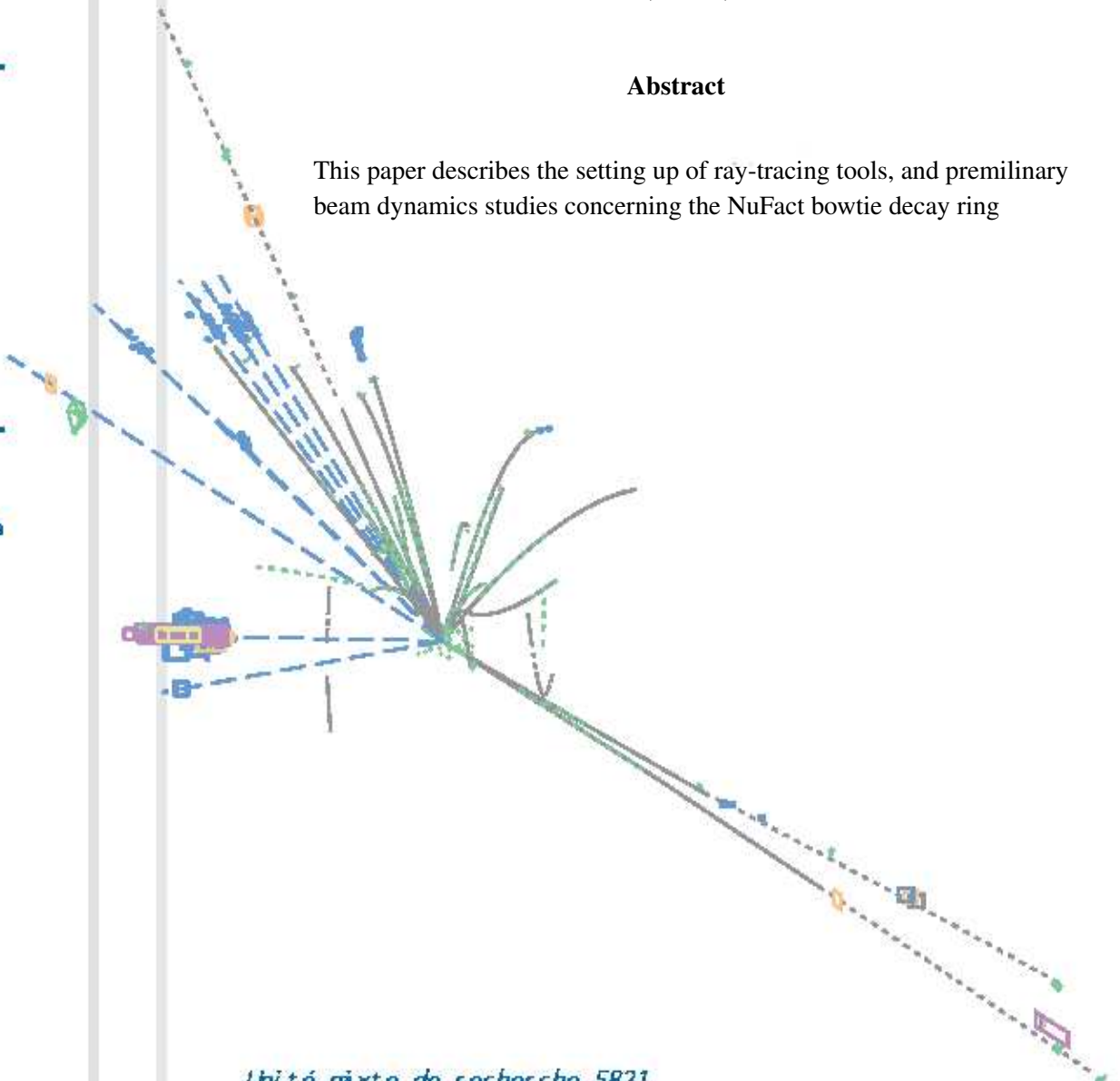
^{*} *Rutherford Appleton Laboratory*

[†] *CNRS IN2P3, LPSC, Grenoble*

[‡] *CEA et IN2P3, LPSC, Grenoble*

Abstract

This paper describes the setting up of ray-tracing tools, and preliminary beam dynamics studies concerning the NuFact bowtie decay ring



Contents

1	Introduction	3
2	Ray-tracing sample results	6
3	Spin tracking	8
	Appendix	9
	Zgoubi data	9
	References	11

1 Introduction

The muon storage ring in the neutrino factory (NuFact in the following) is located at the high energy end of the muon acceleration chain. It delivers the μ^+/μ^- decay neutrinos to physics detectors [1].

The design of concern here is a 20 GeV (upgradable to 50 GeV) bowtie geometry [2] (Fig. 1) which features two decay straight sections, each one aiming at a distant detector, and two return straight sections

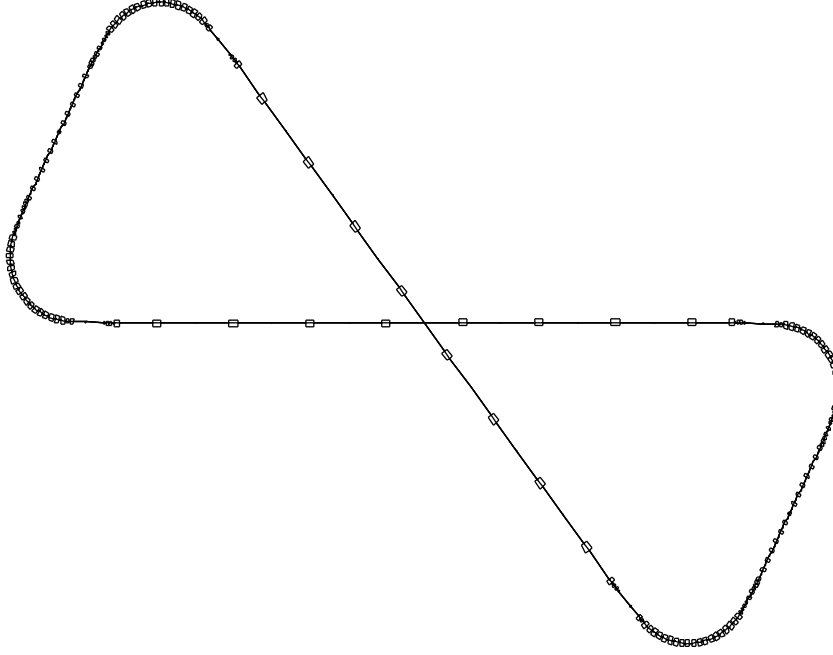


Figure 1: Bowtie decay ring. The two Tuning/Collimation/RF straights are on the left and on the right. The 8-solenoid decay straights are the two others. The four, ten cells arcs are identical.

devoted to tuning, collimation, RF. Geometry and optical parameters are given in Tab. 1 and general behavior is shown in Figs. 2 ; Tab. 1 also displays MAD outputs as obtained from prior translation from the RAL STRING code that has been used for the design, for further checks and comparisons with ray-tracing data. More details can be found in Ref. [3].

Much of this design is derived from the earlier studied isocles triangle decay ring [4, 3, 5]. A particularity is in its being based on solenoid focusing decay straights, which has the virtue of minimizing the betatron amplitudes, compared to equivalent quadrupole focusing. The solenoidal focusing ensures the requested ratio, for the r.m.s. divergences of the 20 GeV muon and the neutrino beam, of 0.1 for an assumed muon normalized r.m.s. emittance of $4800 \pi \text{ mm mr}$ ($3 \pi \text{ cm}$, total).

It is planned to use the ray-racing code Zgoubi for machine design and spin dynamics studies [6], (this is for the sake of accuracy in the representation of magnetic fields - combined function dipoles, solenoids, fringe fields, etc., given the very large beam emittances of concern) thus the goal of the present work is to show how the optics data files have been set up, and to give preliminary results concerning beam and spin dynamics, that show the correct behavior of these, thus allowing further prospects.

Table 1 : Muon storage ring parameters [2].

Energy	(GeV)	Matrix
Circumference	(m)	20
Requested transverse admittance	(π cm, norm.)	1608.8
Requested $\delta p/p$ admittance	(%)	6
Total tunes ν_x/ν_z		± 1
Total chromaticities ξ_x/ξ_z		14.3749 / 12.7882
Phase advances, H/V :	(2π)	-17.7 / -17.7
Arc cell		0.2 / 0.2
production straight		0.69963 / 0.69963
sol./arc match section		0.252525 / 0.205128
tuning straight		1.98279 / 1.284238
Matching conditions :	β_x α_x β_x α_z D_x D'_x	
collimation st centre	8.86984 0 21.08630 0 0 0	
arc input/output	3.78758 0 12.67568 0 0.837046 0	
production st waists	94.21980 0 94.21980 0 0 0	

MAD [7] outputs :

ELEMENT SEQUENCE			H O R I Z O N T A L										V E R T I C A L					
pos.	element	occ.	dist I	betax	alfax	mux	x(co)	px(co)	Dx	Dpx	I	betay	alfay	muy	y(co)	py(co)	Dy	Dpy
no.	name	no.	[m]	[m]	[1]	[2pi]	[mm]	[.001]	[m]	[1]	I	[m]	[1]	[2pi]	[mm]	[.001]	[m]	[1]
ARC TO SOLENOID STRAIGHT MATCHING SECTION :																		
begin	MATCHSEC	1	0.000	3.788	0.000	0.000	0.0000	0.000	0.000	0.000	12.624	0.000	0.000	0.000	0.000	0.000	0.000	0.000
end	MATCHSEC	1	35.000	94.221	-0.001	0.253	0.0000	0.000	0.065	0.043	94.584	-0.014	0.205	0.000	0.000	0.000	0.000	0.000
total length =			35.000000			mux	=		0.252529		muy	=		0.205420				
delta(s) =			0.000000	mm		dmux	=		-0.052988		dmuy	=		-0.067694				
ARC CELL :																		
begin	ARCCELL	1	0.000	5.576	-1.348	0.000	0.0000	0.000	0.994	0.222	9.539	1.955	0.000	0.000	0.000	0.000	0.000	0.000
end	ARCCELL	1	8.200	5.576	-1.348	0.200	0.0000	0.000	0.994	0.222	9.539	1.955	0.200	0.000	0.000	0.000	0.000	0.000
total length =			8.200000			Qx	=		0.200000		Qy	=		0.200000				
delta(s) =			0.000000	mm		Qx'	=		-0.194459		Qy'	=		-0.222650				
10 CELL ARC :																		
begin	ARC10	1	0.000	3.788	0.000	0.000	0.0000	0.000	0.000	0.000	12.624	0.000	0.000	0.000	0.000	0.000	0.000	0.000
end	ARC10	1	82.000	3.788	0.000	2.000	0.0000	0.000	0.000	0.000	12.624	-0.004	2.000	0.000	0.000	0.000	0.000	0.000
total length =			82.000000			mux	=		2.000000		muy	=		2.000000				
delta(s) =			0.000000	mm		dmux	=		-1.944237		dmuy	=		-2.236326				
TUNING SECTION :																		
begin	TUNINGSE	1	0.000	3.788	0.000	0.000	0.0000	0.000	0.000	0.000	12.624	0.000	0.000	0.000	0.000	0.000	0.000	0.000
end	TUNINGSE	1	145.246	3.788	0.000	1.983	0.0000	0.000	0.005	-0.024	12.624	0.000	1.285	0.000	0.000	0.000	0.000	0.000
total length =			145.245748			mux	=		1.982785		muy	=		1.285053				
delta(s) =			0.000000	mm		dmux	=		-4.349365		dmuy	=		-3.028322				
SOLENOID STRAIGHT :																		
begin	SOLESTRA	1	0.000	94.000	0.000	0.000	0.0000	0.000	0.000	0.000	94.000	0.000	0.000	0.000	0.000	0.000	0.000	0.000
end	SOLESTRA	1	425.156	93.698	-0.057	0.700	0.0000	0.000	0.000	0.000	93.698	-0.057	0.700	0.000	0.000	0.000	0.000	0.000
total length =			425.155626			mux	=		0.699752		muy	=		0.699752				
delta(s) =			0.000000	mm		dmux	=		-0.714953		dmuy	=		-0.714953				
FULL BOWTIE :																		
begin	BOWTIE	1	0.000	114.889	-0.329	0.000	0.0000	0.000	0.000	0.000	98.535	0.033	0.000	0.000	0.000	0.000	0.000	0.000
end	BOWTIE	1	1608.803	119.269	-0.301	14.400	0.0000	0.000	0.000	0.000	97.094	-0.086	12.751	0.000	0.000	0.000	0.000	0.000
total length =			1608.802747			Qx	=		14.399904		Qy	=		12.751446				
delta(s) =			0.000000	mm		Qx'	=		-17.691073		Qy'	=		-17.663926				
alfa =			0.540925E-02			betax(max)	=		136.836657		betay(max)	=		130.757453				
gamma(tr) =			13.596636			Dx(max)	=		1.290411		Dy(max)	=		0.001194				

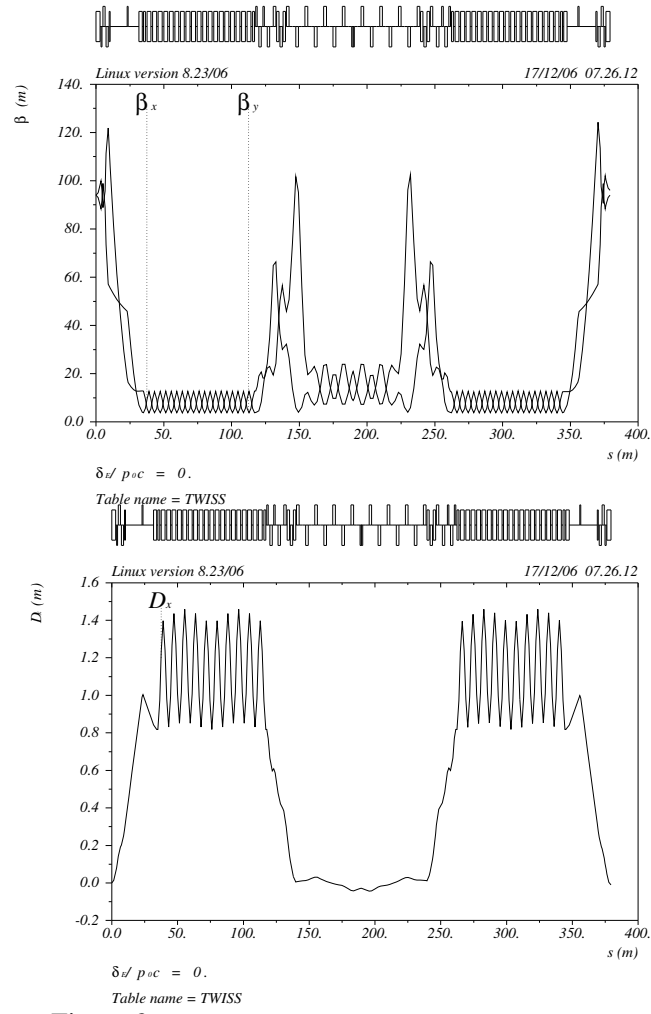
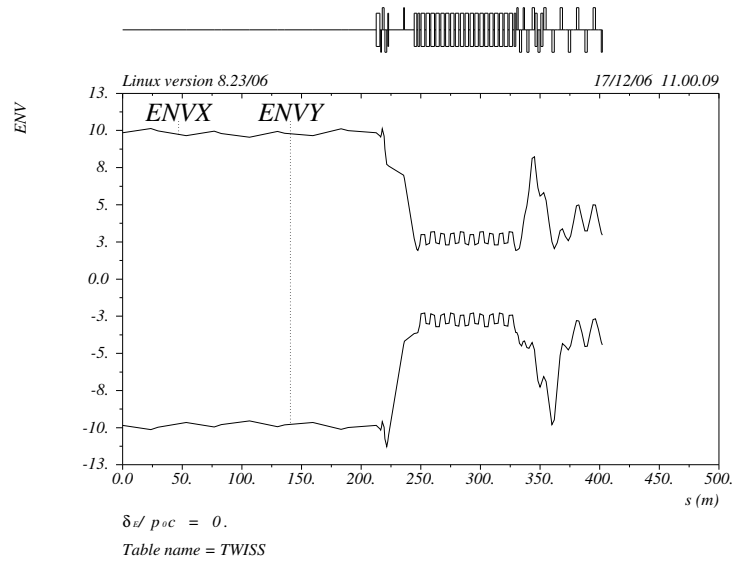


Figure 2: Optical functions in half the bowtie ring.

Figure 3: Beam envelopes ($\epsilon_{x,z} = 1$) in a quarter of the bowtie, from middle of production straight to middle of tuning section.

2 Ray-tracing sample results

The essential of Zgoubi data file is given in App. 3. The subparts of the bowtie ring are very near, in geometry and optical tunings, to the triangle ones, therefore it can usefully referred to Ref. [3] for more details.

The Zgoubi optics file is obtained by direct translation from a MAD “survey” output. The agreement between transport type and ray-tracing outputs is straightforward as long as pure dipoles and other higher order multipoles are concerned, which is not the case here : the use of combined function dipoles in the arcs, in addition to the presence of fringe fields, requires positioning adjustments ; the superimposition of a sextupole component for chromaticity correction requires additional adjustment of both closed orbit and tuning, minor though ; the long fall-offs of solenoid fields requires strength adjustment.

Zeroing of the horizontal closed orbit is a first effect of dipole positioning adjustment. A first approach is shown in Fig. 4, it can still be improved by better adjustment of all dipoles.

Beam envelopes obtained using STRING’s strengths are shown in Fig. 5, they are in excellent agreement with transport methods (Fig. 3), which shows that little gradient adjustments will be needed to get identical ray-tracing focusing conditions.

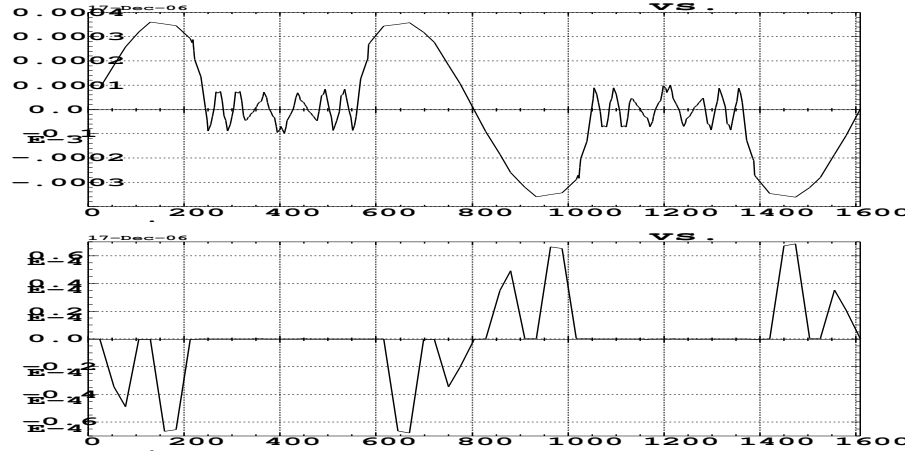


Figure 4: Residual geometrical closed orbits. The (negligible) vertical one is due to residual coupling in the solenoid.

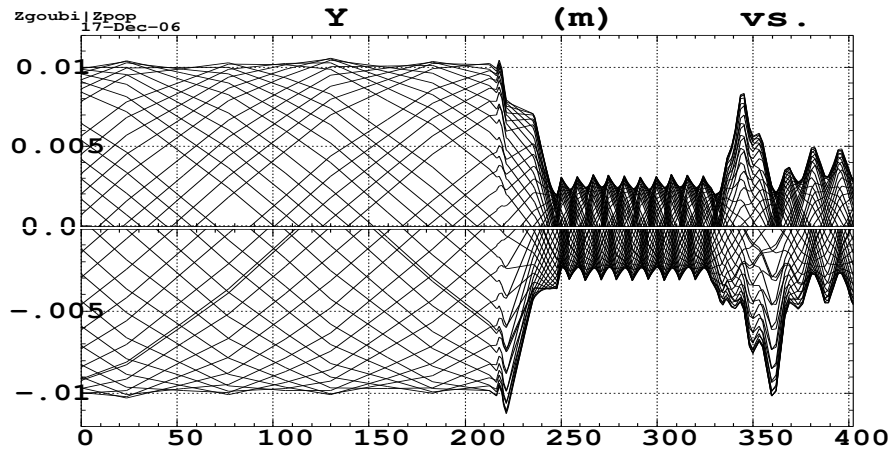


Figure 5: Horizontal (top) and vertical (bottom) beam envelopes ($\epsilon_{x,z} = 1$) in the bowtie ring, from ray-tracing.

Focusing properties computed from ray-tracing are the following :

Middle of tuning straight :

Beam matrix	(beta/-alpha/-alpha/gamma)	and	periodic	dispersion	(MKSA units)
7.59592	-0.228524	0.00000	0.00000	0.00000	-3.021585E-02
-0.228524	9.025691E-02	0.00000	0.00000	0.00000	-4.713025E-04
0.00000	0.00000	21.9151	-4.881490E-02	0.00000	0.00000
0.00000	0.00000	-4.8815E-02	2.900786E-02	0.00000	0.00000

Arc input/output :

3.78813	1.142890E-04	0.00000	0.00000	0.00000	0.818142
1.142890E-04	0.263982	0.00000	0.00000	0.00000	-3.255178E-05
0.00000	0.00000	12.6777	1.386475E-03	0.00000	0.00000
0.00000	0.00000	1.386475E-03	7.887899E-02	0.00000	0.00000

Middle of the production section :

Beam matrix	(beta/-alpha/-alpha/gamma)	and	periodic	dispersion	(MKSA units)
80.893747	-0.176882	0.000000	0.000000	0.000000	-0.018887
-0.176882	0.012749	0.000000	0.000000	0.000000	-0.000278
0.000000	0.000000	94.896068	-0.109185	0.000000	0.000003
0.000000	0.000000	-0.109185	0.010663	0.000000	0.000000

Betatron tunes (fractional) :

$$\text{NU}_Y = 0.34725094 \quad \text{NU}_Z = 0.76608261$$

Chromaticities :

$$d\text{Nu}_y / dp/p = -14.393117 \quad d\text{Nu}_z / dp/p = -16.228313$$

Comparison with data in Tab. 1 shows satisfactory agreement in optical functions at the various observation points ; this can be improved by adjusting the quadrupoles (in the matching and tuning sections) whereas no attempt has been done on that. The difference in fractional part of tunes with design values (Tab. 1) is very small (0.027 horizontal and 0.022 vertical) although the sole arc cells have been tuned to their exact requested phase advance, 0.2. This small difference can easily be zeroed by adjustment of the tuning section quadrupoles. Chromaticities as well are in good agreement.

Large amplitude tracking samples below have the mere goal of giving a rapid idea of expectable admittance. They are clearly satisfactory and justify further inspection, including 4-D motion, beam transmission, etc., as performed in the triangle ring case [3].

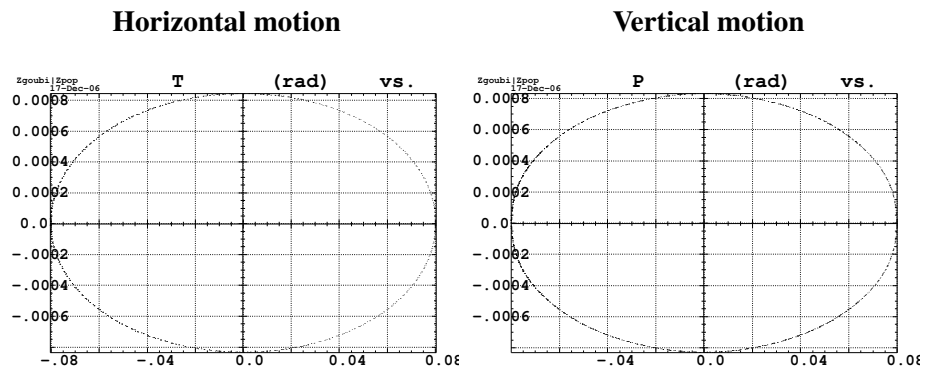


Figure 6: Phase space trajectories of an on-momentum particle launched on $\epsilon_x/\pi \approx 1.5$ cm (left) or $\epsilon_z/\pi \approx 1.5$ cm (right) invariant. 1000 turns in the ring.

3 Spin tracking

The preliminary data installations and tests above show a good behavior of particle dynamics computation, allowing further spin dynamics studies using ray-tracing method. Static mode can be considered (search for spin closed orbit, resonance strength computation, etc., the beam staying at constant distance from the resonance, see methods in Ref. [6] for instance), as well as resonance crossing mode if using “CAVITE” for acceleration (although no acceleration is going to occur in reality) which would for instance yield precise estimate of the resonant energy, or as well stationary bucket mode (see example in Section 3 of Zgoubi users’ guide [8]).

Preliminary checks show a good symplecticity of the spin tracking using the integration steps given in App. 3. This should be checked further, depending on transverse amplitudes in particular. The spin generator in Zgoubi allows creating all sort of initial conditions, random or not, whereas the analysis/graphic interface software zpop [8] allows all sorts of spin analysis, spin motion plots.

The Figure below shows for illustration a 1000-turn tracking in the defect-free bowtie with tunig conditions addressed above (in particular, no vertical closed orbit defect).

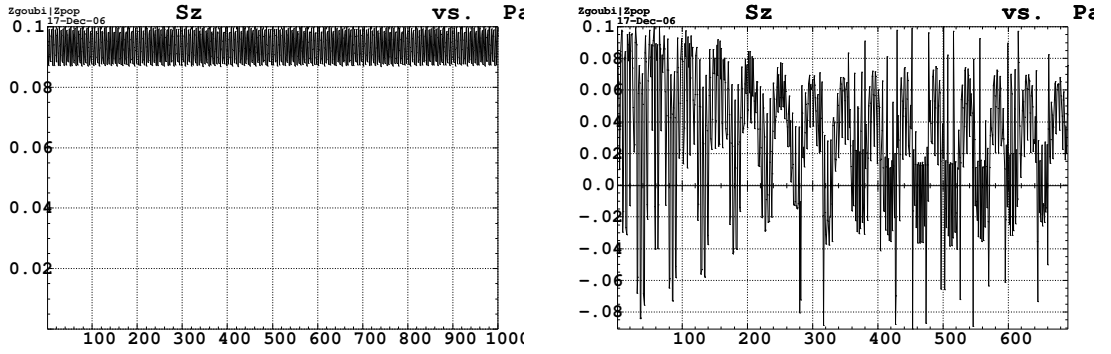


Figure 7: Vertical component of the spin, versus turn number, observed in the middle of the production straight. Left : $\epsilon_x/\pi \approx 1.5$ cm, $\epsilon_z/\pi = 0$, right : $\epsilon_x/\pi \approx 0$ cm, $\epsilon_z/\pi \approx 1.5$ cm.

On the other hand, it has been checked that all along the tracking range, $S_x^2 + S_y^2 + S_z^2 = 1$, at computer precision, which is an indication of good symplecticity, and of small enough integration step size.

Appendix

Zgoubi data

Object definition and storage options :

```
'OBJET'
67064.301000
6
.001 .001 .001 .001 0. .000001
0. 0. 0. 0. 0. 1.
'PARTICUL'
105.66 1.60217733D-19 1. 0. 0.
'SPNTRK'
3
'SPNPRNL'
zgoubi.spn
'SPNPRT'
'PICKUPS'
1
DRIF
'FAISTORE'
b_zgoubi.fai DRIF #S #E
1
```

“PARTICUL” allows input of the muon mass and charge for γ computation, and of the gyromagnetic factor, two quantities necessary for spin tracking.

“PICKUPS” is used for computation of closed orbit.

“FAISTORE” allows storage of particle coordinates for phase-space plots.

“SPNTRK” requests spin tracking while the option 3 sets all initial spins upright, whereas “SPNPRNL” causes storage of spin components.

Solenoid cell :

```
'DRIFT' DRIF D1
2360.0000
'SOLENOID' SOLE SOLP
0 .solenoid
594.4453 20. 42.17
600. 600.
1. Soleno SOLP
1 0. 0. 0.
'DRIFT' DRIF D1
2360.0000
```

Solenoid to arc matching section :

```
'CHANGREF'
0. 0. -1.111652714
'CHANGREF'
0. 0. 0.96109104 0.0
'MULTIPOL' SBEN BMS
0 .Dip
299.9812 10.00 8.67454379 0.33532151 0. 0. 0. 0. 0. 0. 0. 0. 0.
20.00 11.20 1.00 1.00 1.00 1.00 0.00 0. 0. 0. 0.
6 .015527 3.874961 -2.362230 2.978209 12.604429 15.025689
20.00 11.20 1.00 1.00 1.00 1.00 0.00 0. 0. 0. 0.
6 .015527 3.874961 -2.362230 2.978209 12.604429 15.025689
0. 0. 0. 0. 0. 0. 0. 0. 0. 0. 0.
#120|300|120 Dip BMS
2 0. 0. 0.
'CHANGREF'
0. -0.96109104 0.0
'CHANGREF'
0. 0. -1.111652714
'DRIFT' DRIF D2
60.0000
'MULTIPOL' QUAD QD1
```

```
0 .Quad
80.0000 10.00 0.00 -6.5863675 0. 0. 0. 0. 0. 0. 0. 0. 0.0
9.0 9.0 1.00 0.00 0.00 0.00 0.00 0. 0. 0. 0.
6 .1122 6.2671 -1.4982 3.5882 -2.1209 1.723 arc
9.0 9.0 1.00 0.00 0.00 0.00 0.00 0. 0. 0. 0.
6 .1122 6.2671 -1.4982 3.5882 -2.1209 1.723 arc
0. 0. 0. 0. 0. 0. 0. 0. 0. 0.
#30|80|30 Quad QD1
1 0. 0. 0.
'DRIFT' DRIF D2
60.0000
'MULTIPOL' QUAD QF1
0 .Quad
160.0000 10.00 0.00 7.7113265 0. 0. 0. 0. 0. 0. 0. 0. 0.0
9.0 9.0 1.00 0.00 0.00 0.00 0.00 0. 0. 0. 0.
6 .1122 6.2671 -1.4982 3.5882 -2.1209 1.723 arc
9.0 9.0 1.00 0.00 0.00 0.00 0.00 0. 0. 0. 0.
6 .1122 6.2671 -1.4982 3.5882 -2.1209 1.723 arc
0. 0. 0. 0. 0. 0. 0. 0. 0. 0.
#30|160|30 Quad QF1
1 0. 0. 0.
'DRIFT' DRIF D3
70.0000
'MULTIPOL' QUAD QD2
0 .Quad
160.0000 10.00 0.00 -6.0648503 0. 0. 0. 0. 0. 0. 0. 0. 0.0
9.0 9.0 1.00 0.00 0.00 0.00 0.00 0. 0. 0. 0.
6 .1122 6.2671 -1.4982 3.5882 -2.1209 1.723 arc
9.0 9.0 1.00 0.00 0.00 0.00 0.00 0. 0. 0. 0.
6 .1122 6.2671 -1.4982 3.5882 -2.1209 1.723 arc
0. 0. 0. 0. 0. 0. 0. 0. 0. 0.
#30|160|30 Quad QD2
1 0. 0. 0.
'DRIFT' DRIF D4
70.0000
'CHANGREF'
0. 0. -0.190643112
'CHANGREF'
0. 3.54677553E-02 0.0
'MULTIPOL' SBEN BMB
0 .Dip
79.9999 10.00 5.57866005 0. 0. 0. 0. 0. 0. 0. 0. 0.0
20.00 11.20 1.00 1.00 1.00 1.00 0.00 0. 0. 0. 0.
6 .015527 3.874961 -2.362230 2.978209 12.604429 15.025689
20.00 11.20 1.00 1.00 1.00 1.00 0.00 0. 0. 0. 0.
6 .015527 3.874961 -2.362230 2.978209 12.604429 15.025689
0. 0. 0. 0. 0. 0. 0. 0. 0. 0.
#120|80|120 Dip BMB
2 0. 0. 0.
'CHANGREF'
0. -3.54677553E-02 0.0
'CHANGREF'
0. 0. -0.190643112
'DRIFT' DRIF D5
1250.0000
'MULTIPOL' QUAD QF2
0 .Quad
80.0000 10.00 0.00 6.1619058 0. 0. 0. 0. 0. 0. 0. 0. 0.0
9.0 9.0 1.00 0.00 0.00 0.00 0.00 0. 0. 0. 0.
6 .1122 6.2671 -1.4982 3.5882 -2.1209 1.723 arc
9.0 9.0 1.00 0.00 0.00 0.00 0.00 0. 0. 0. 0.
6 .1122 6.2671 -1.4982 3.5882 -2.1209 1.723 arc
0. 0. 0. 0. 0. 0. 0. 0. 0. 0.
#30|80|30 Quad QF2
1 0. 0. 0.
'DRIFT' DRIF D6
800.0000
'CHANGREF'
0. 0. 0.078982232
'CHANGREF'
0. -5.48572737E-02 0.0
'MULTIPOL' SBEN BMR
0 .Dip
239.9999 10.00 -0.77040116 -0.77762050 0. 0. 0. 0. 0. 0. 0. 0. 0.0
20.00 11.20 1.00 1.00 1.00 1.00 0.00 0. 0. 0. 0.
6 .015527 3.874961 -2.362230 2.978209 12.604429 15.025689
20.00 11.20 1.00 1.00 1.00 1.00 0.00 0. 0. 0. 0.
6 .015527 3.874961 -2.362230 2.978209 12.604429 15.025689
0. 0. 0. 0. 0. 0. 0. 0. 0. 0.
#120|240|120 Dip BMR
2 0. 0. 0.
'CHANGREF'
0. 5.48572737E-02 0.0
'CHANGREF'
0. 0. 0.078982232
'DRIFT' DRIF D7
90.0000

Arc cell :

'DRIFT' DRIF D8
120.0000
```

Tuning section, up to first DS dipole :

```
'DRIFT' DRIF D9
80.0000
'MULTIPOL' QUAD QF3
0 .Quad
110.0000 10.00 0.00 6.6368978327 0. 0. 0. 0. 0. 0. 0. 0. 0. 0.
9.0 9.0 1.00 0.00 0.00 0.00 0.00 0. 0. 0. 0. 0.
6 .1122 6.2671 -1.4982 3.5882 -2.1209 1.723 arc
9.0 9.0 1.00 0.00 0.00 0.00 0.00 0. 0. 0. 0. 0.
6 .1122 6.2671 -1.4982 3.5882 -2.1209 1.723 arc
0. 0. 0. 0. 0. 0. 0. 0. 0. 0. 0.
#30|110|30 Quad QF3
1 0. 0. 0.
'DRIFT' DRIF D10
120.0000
'MULTIPOL' QUAD QD3
0 .Quad
180.0000 10.00 0.00 -5.8842217697 0. 0. 0. 0. 0. 0. 0. 0. 0. 0.
9.0 9.0 1.00 0.00 0.00 0.00 0.00 0. 0. 0. 0. 0.
6 .1122 6.2671 -1.4982 3.5882 -2.1209 1.723 arc
9.0 9.0 1.00 0.00 0.00 0.00 0.00 0. 0. 0. 0. 0.
6 .1122 6.2671 -1.4982 3.5882 -2.1209 1.723 arc
0. 0. 0. 0. 0. 0. 0. 0. 0. 0. 0.
#30|180|30 Quad QD3
1 0. 0. 0.
'DRIFT' DRIF D10
120.0000
'MULTIPOL' QUAD QF4
0 .Quad
110.0000 10.00 0.00 6.1766221221 0. 0. 0. 0. 0. 0. 0. 0. 0. 0.
9.0 9.0 1.00 0.00 0.00 0.00 0.00 0. 0. 0. 0. 0.
6 .1122 6.2671 -1.4982 3.5882 -2.1209 1.723 arc
9.0 9.0 1.00 0.00 0.00 0.00 0.00 0. 0. 0. 0. 0.
6 .1122 6.2671 -1.4982 3.5882 -2.1209 1.723 arc
0. 0. 0. 0. 0. 0. 0. 0. 0. 0. 0.
#30|110|30 Quad QF4
1 0. 0. 0.
'DRIFT' DRIF D11
210.0000
'MULTIPOL' QUAD QD4
0 .Quad
180.0000 10.00 0.00 -3.1251964266 0. 0. 0. 0. 0. 0. 0. 0. 0. 0.
9.0 9.0 1.00 0.00 0.00 0.00 0.00 0. 0. 0. 0. 0.
6 .1122 6.2671 -1.4982 3.5882 -2.1209 1.723 arc
9.0 9.0 1.00 0.00 0.00 0.00 0.00 0. 0. 0. 0. 0.
6 .1122 6.2671 -1.4982 3.5882 -2.1209 1.723 arc
0. 0. 0. 0. 0. 0. 0. 0. 0. 0. 0.
#30|180|30 Quad QD4
1 0. 0. 0.
'DRIFT' DRIF D7
90.0000
'DRIFT' DRIF D7
```

References

- [1] Muon storage rings for the neutrino factory, C. Johnstone et als., Procs. EPAC 2006 Conf.
- [2] Bowtie20, 20 GeV, μ^+ and μ^- , Bow-tie, Storage Rings, G. Rees, RAL, unpublished (2006).
- [3] NuFact muon storage ring : study of a triangle design based on solenoid focusing decay straights, F. Méot and G. Rees, report IN2P3 LPSC 06-38 (2006).
- [4] Stormu20, 20 GeV, μ^+ and μ^- , Isosceles Triangle, Storage Rings, G. Rees, RAL, unpublished (2005).
- [5] Study of defacts in the NuFact muon storage ring, ISS-NuFact report, to be published (2007)
NuFact muon storage ring : study of defects, F. Méot, report IN2P3 LPSC, to be published (2007).
- [6] A numerical method for combined spin tracking and ray-tracing of charged particles, F. Méot, NIM A313 (1992) 492-500.
- [7] The MAD Program, User's Reference Manual, H. Grote, F. C. Iselin, CERN/SL/90-13 (AP) (Rev. 5), CERN, 29 April 1996.
- [8] Zgoubi users' guide - Version 4, F. Méot and S. Valero, FNAL Report FERMILAB-TM-2010, Aug. 1997, CEA DSM DAPNIA/SEA-97-13, Saclay, Oct. 1997.